Long-lived Heavy Neutrino Searches at Colliders

Kechen Wang (王科臣)
Wuhan University of Technology (武汉理工大学)

2023年BESIII 新物理研讨会

Wuhan U, Wuhan, October 14, 2023

Based on [王泽人、张敬民、毛英男、王科臣，hep-ph/2305.03908, JHEP 09 (2021) 026; PRD 101 (2020) no.7, 075046]

OUTLINE

LLP Searches @ Colliders

***N* Production & Limits @ Colliders**

Long-lived *N* Studies

Discussion

Theoretical Motivations

LLP: Relatively long lifetime or equivalently long decay length

New particles become long-lived because of:
→ feeble couplings to SM particles
→ phase space suppression
→ approximate symmetry
→ heavy mediators, ...

The discovery of LLPs could explain some fundamental problems:
neutrino mass, dark matter, baryogenesis, naturalness, ...

LLP searches are important ways to BSM physics !

Idea of LLP searches @ colliders

When a LLP produced at 0 (usually the IP),

Probability of still existing (does not decay) at L

$$P(L) = e^{-L/\lambda}$$

where decay length in the lab. frame

$$\lambda = \beta\gamma\, c\tau = \left(\frac{p}{m}\right)\ (c\tau)$$

Kinematics lifetime in the rest frame

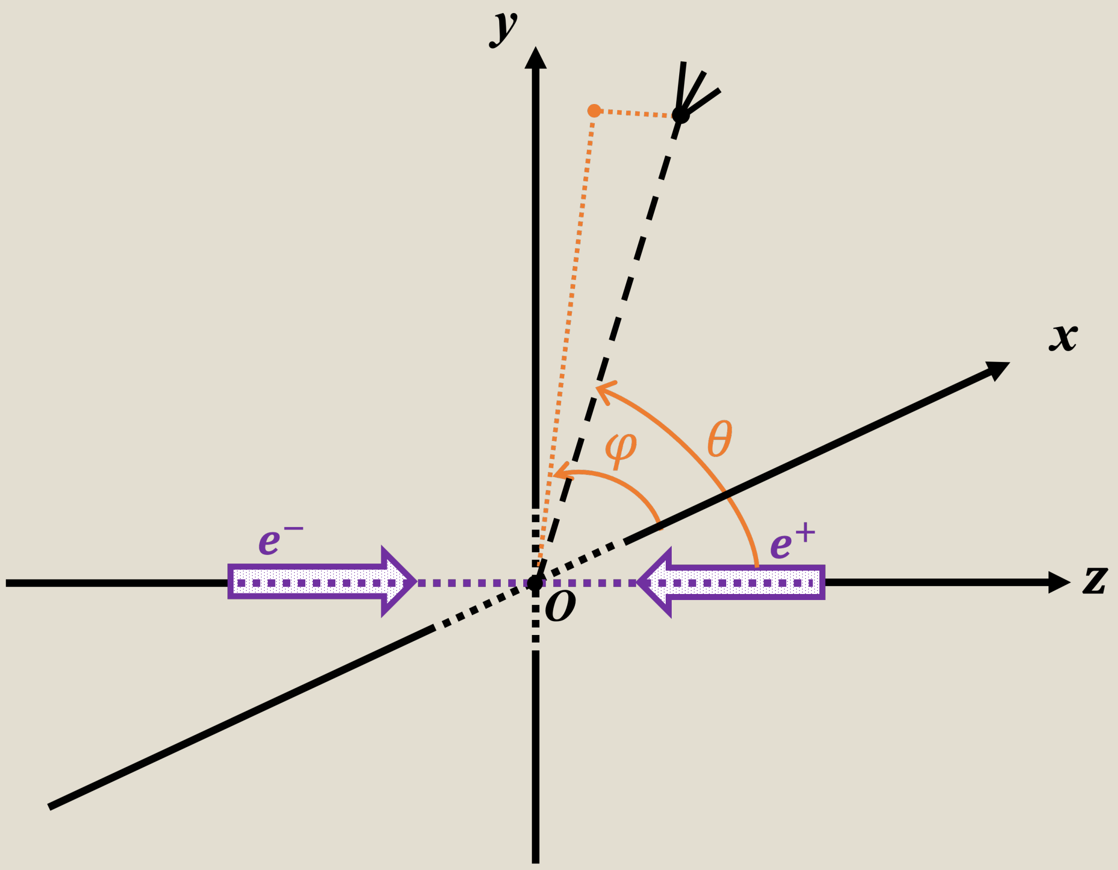

Idea of LLP searches @ colliders

Probability of decaying between L_1 and L_2 ($L_1 < L_2$)

$$P(\Delta L) = e^{-L_1/\lambda} - e^{-L_2/\lambda}$$

L_1 and L_2 :
determined by the detector (position, shape, volume, ...) & LLP's moving direction

Exponential Decay

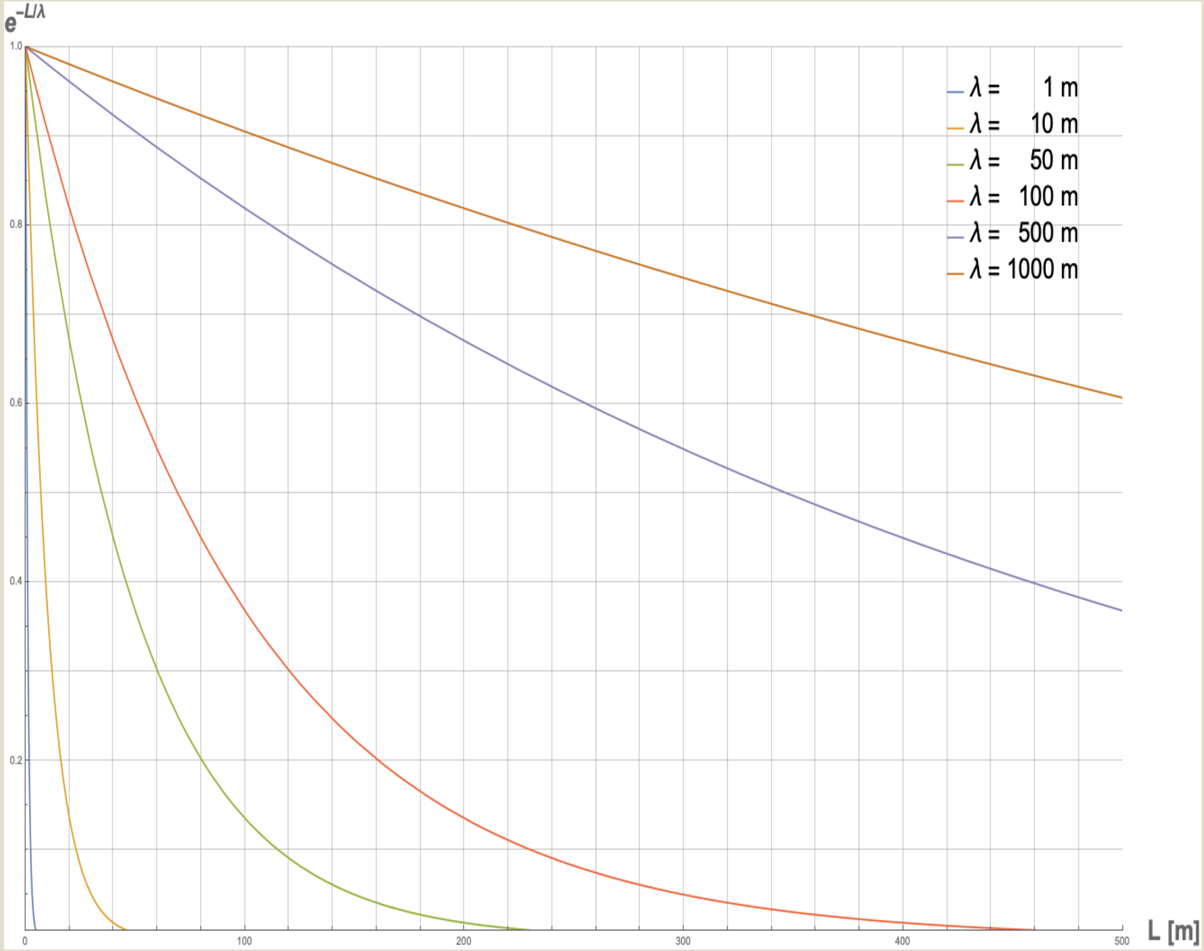

Idea of LLP searches @ colliders

$$\boldsymbol{N_{\text{exp}} = N_{\text{pro}} \cdot P \cdot \text{Br} \cdot \epsilon}$$

\# of LLPs produced

probability of decaying inside the detector's fiducial volume

Branching ratio of LLP decaying into visible final state

detector efficiency

expected # of signal events:
depends on theory model parameters (mass, lifetime, kinematics) & geometry and performance of detector (position, shape, volume, efficiency)

@ *ee* vs. *pp*
***ee*:** high lum., clean environment, trigger, EW prod., transverse direction, recoil strategy
***pp*:** forward direction

Signatures of LLPs in ND

When $\lambda \sim \mathcal{O}(1)$ m,

Mainly decay inside the near detector

Appear as displaced vertex

Various final states depending on different decay products

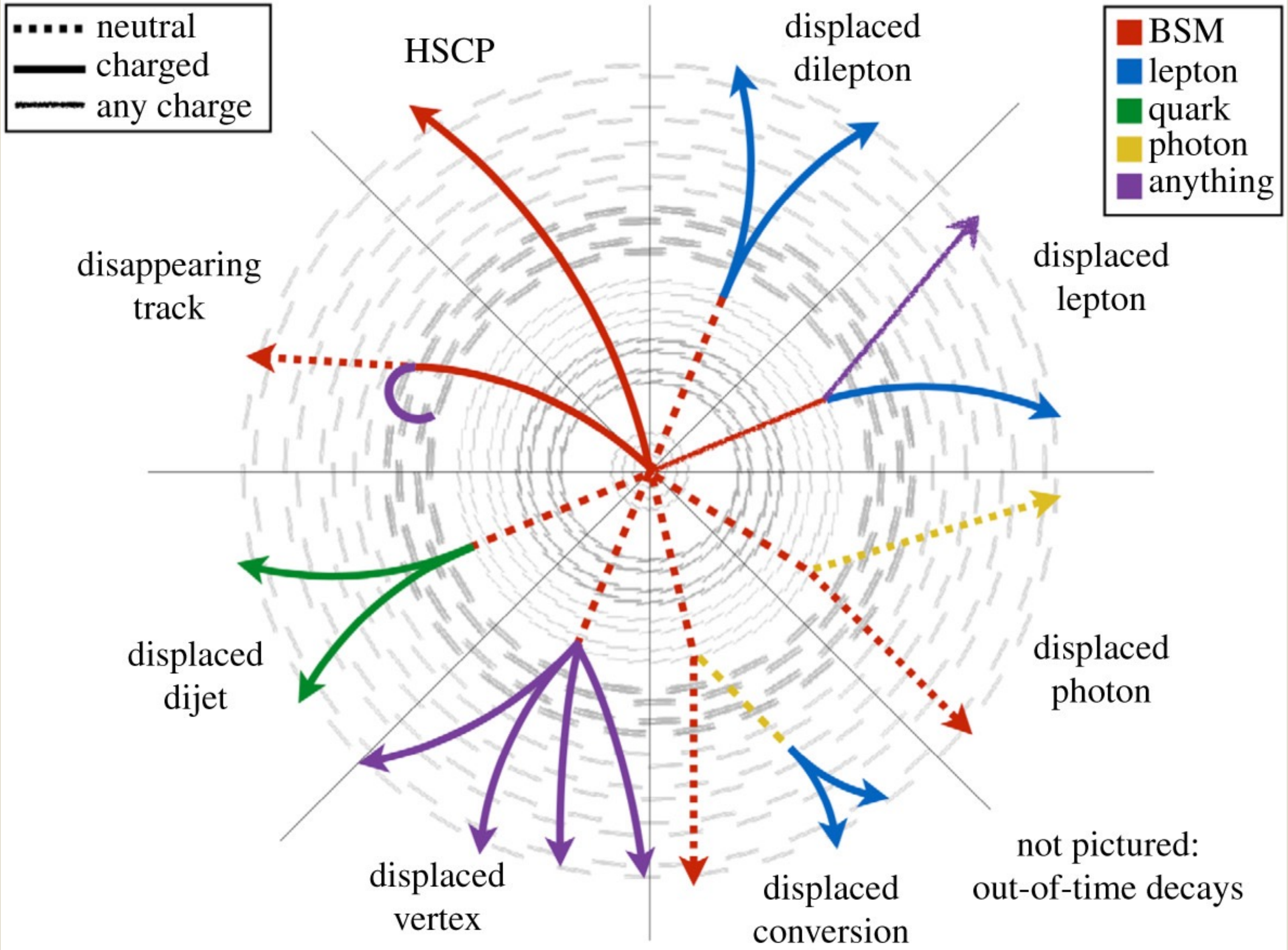

Figure from [A. De Roeck, Phil. Trans. Roy. Soc. Lond. A 377, 20190047 (2019)]

Signatures of LLPs in FD

When $\lambda \sim \mathcal{O}(100)$ m,

Mainly travel through and acts as missing energy in the near detector.

Far detector is more likely to observe the decay process, and reconstruct the time, position, direction, momentum, mass, etc.

Far detector can enhance the discovery potential for LLPs with very long decay length.

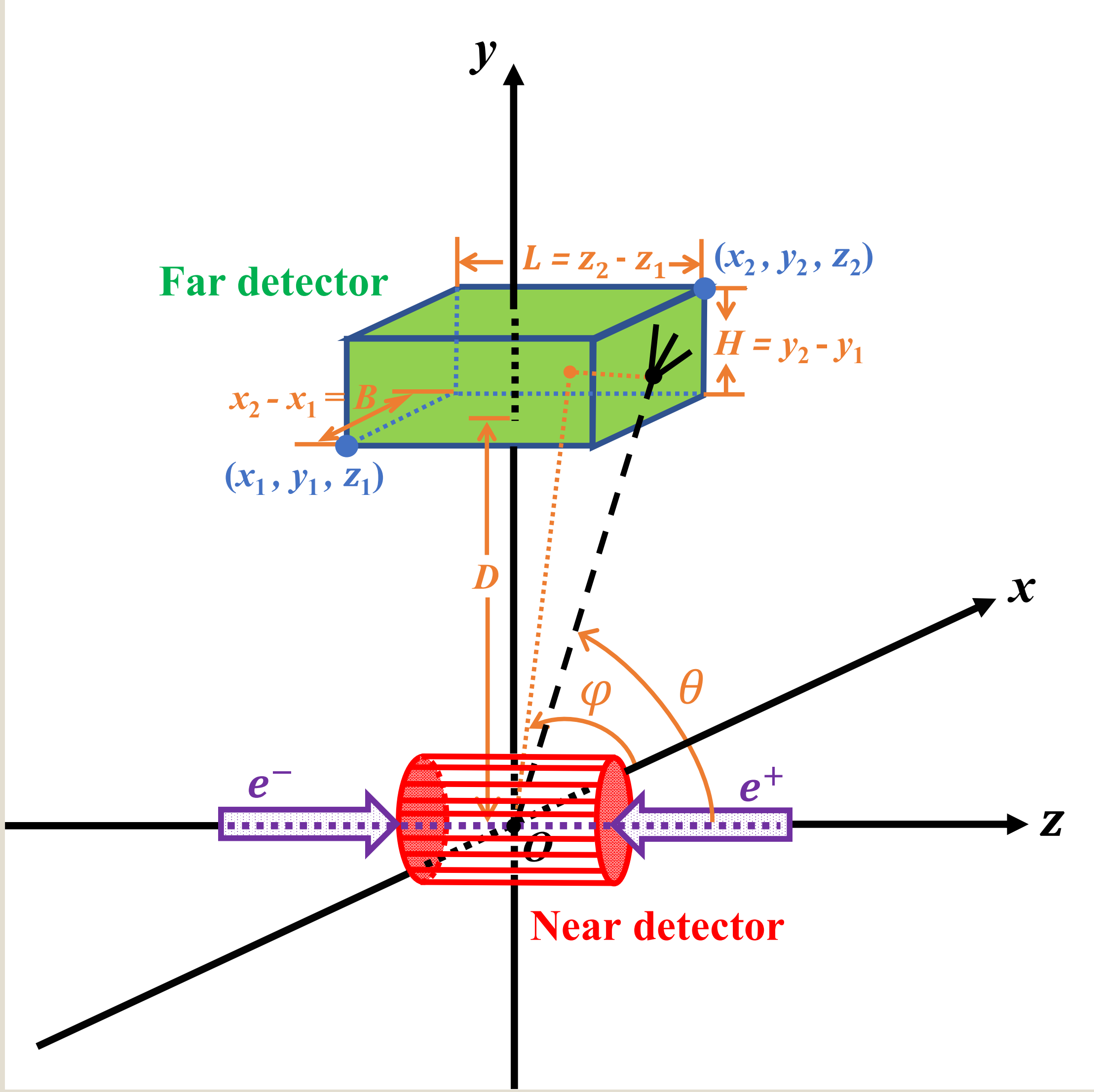

Heavy Neutrino Models

Discovery of neutrino oscillations => neutrinos have mass
→ In SM, neutrinos are massless
→ A window to BSM physics

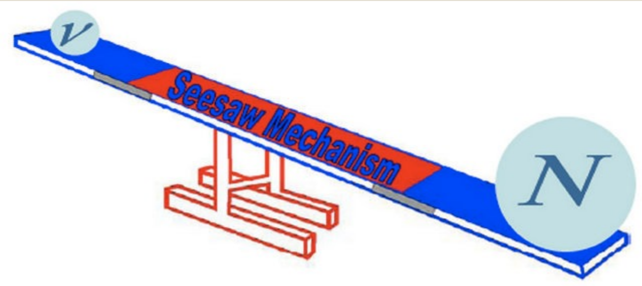

Type-I see-saw: Singlet (Sterile) Fermions

$$\boxed{-\mathcal{L} \;=\; h_{\ell\alpha}\bar{L}_\ell\widetilde{\Phi}N_\alpha + \frac{1}{2}M_{N_{\alpha\beta}}\bar{N}^C_\alpha N_\beta + \mathrm{H.c.}}$$

$$\boxed{M_\nu \;=\; \begin{pmatrix} 0 & M_D \\ M_D^\mathsf{T} & M_N \end{pmatrix}} \qquad M_\nu \;\simeq\; -M_D M_N^{-1} M_D^\mathsf{T}$$

$$V_{\ell N_\alpha} \sim M_D M_N^{-1}$$

Interactions: [0901.3589]

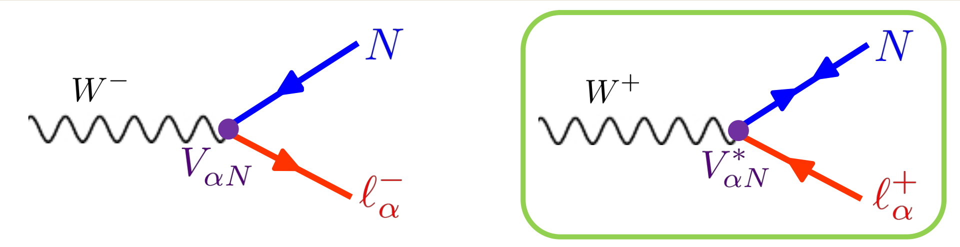

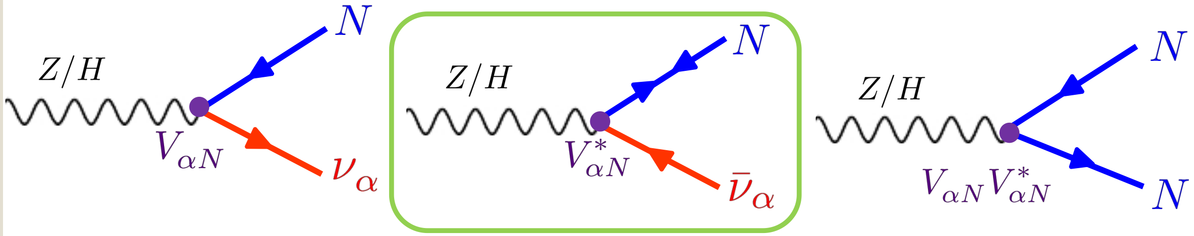

Simplified model with assumption for collider searches:
Assumption: Dirac/Majorana, # of *N*s
Free parameters: m_N, $|V_{Ne}|^2$, $|V_{N\mu}|^2$, $|V_{N\tau}|^2$

N Production @ *pp* Colliders

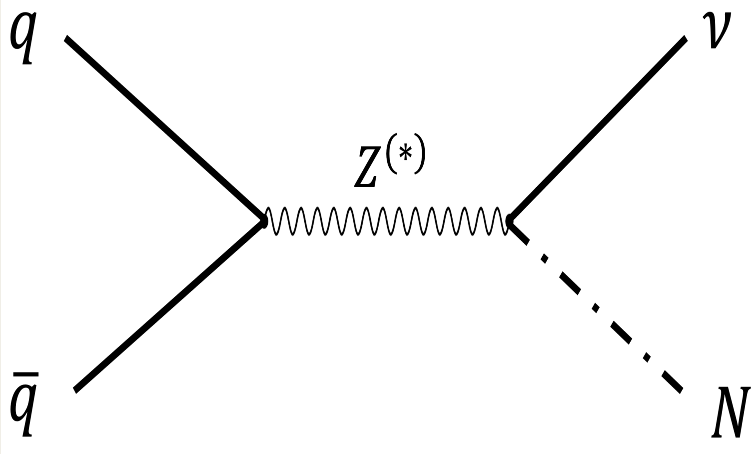

almost unobserved
(l^+l^- or $l^\pm$+MET suffer from huge BG)

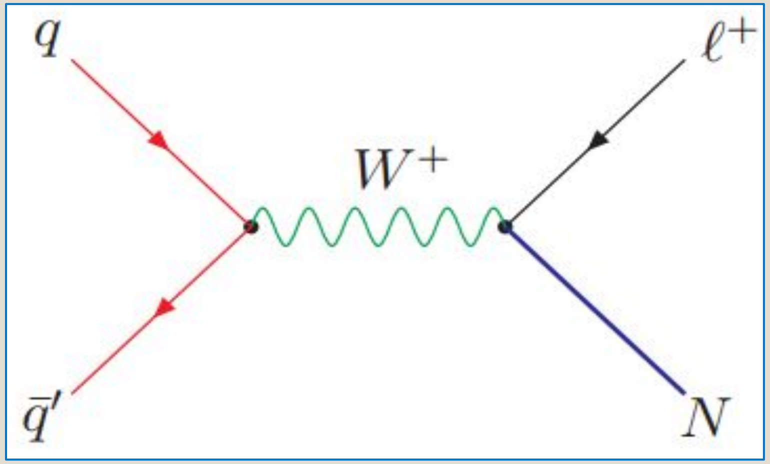

mostly studied, can confirm LNV
(important for m_N < 1 TeV)
[L. Bai, Y. Mao and **K. Wang**, PRD 107 (2023) no. 9, 095008]

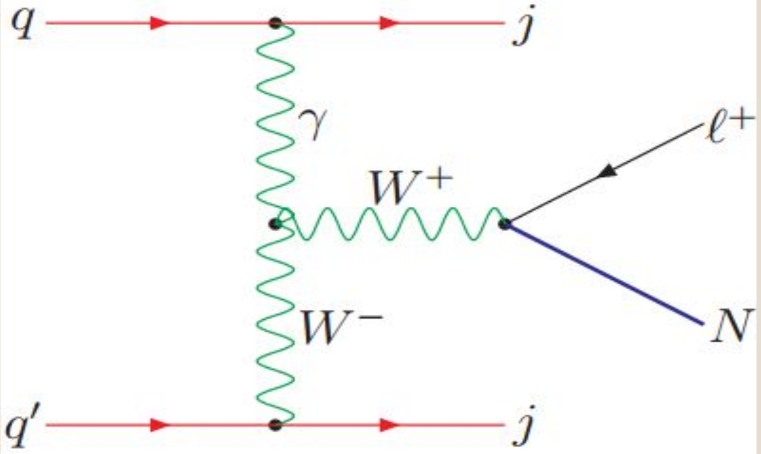

can confirm LNV
(More important for m_N > 1 TeV)

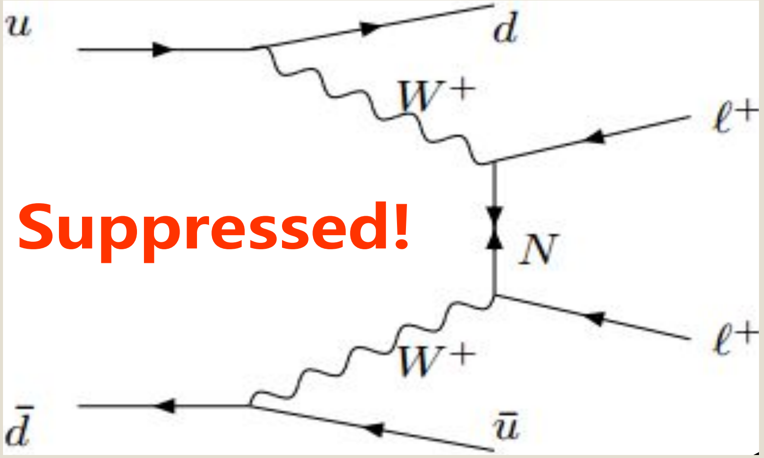

can confirm LNV
(no resonance enhancement)

N Production @ ee Colliders

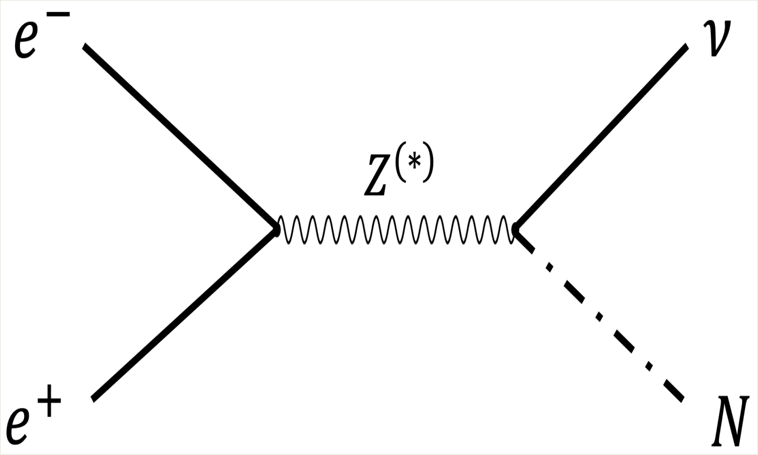

Mostly studied @ Z-pole
(important for $m_N < m_Z$)

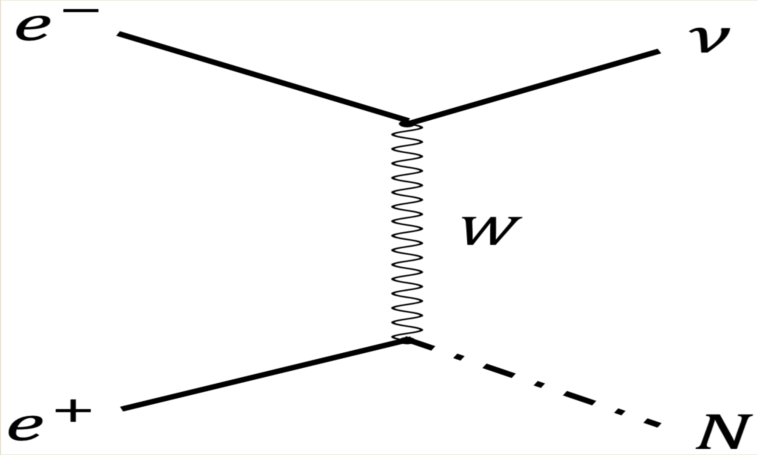

contribute to signal
(important for large m_N)

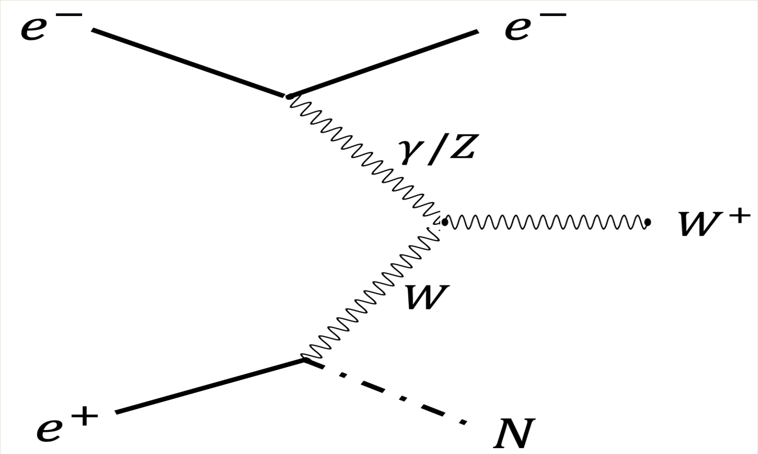

can confirm LNV
(important for large m_N , need large $\sqrt{s}$)

N Production @ *pe* Colliders

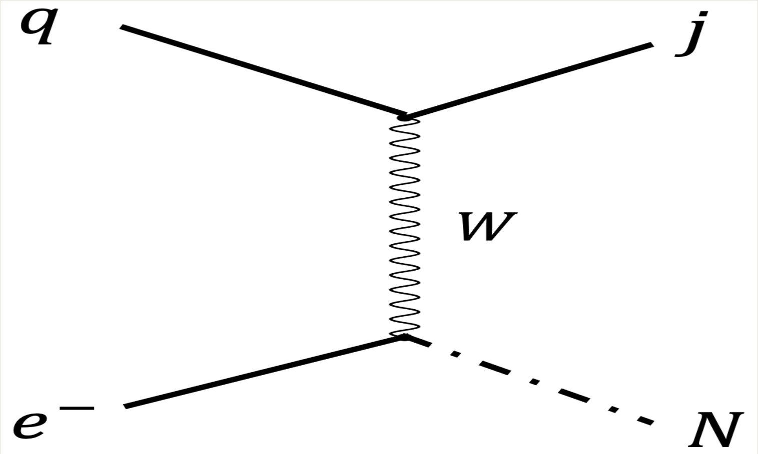

Mostly studied, can confirm LNV
(sensitive to wide range, esp. $m_N > m_Z$)
[H. Gu, Y. Mao, H. Sun and **K. Wang**, JHEP 09 (2023) 152]
[H. Gu and **K. Wang**, PRD 106 (2022) no. 1, 015006]

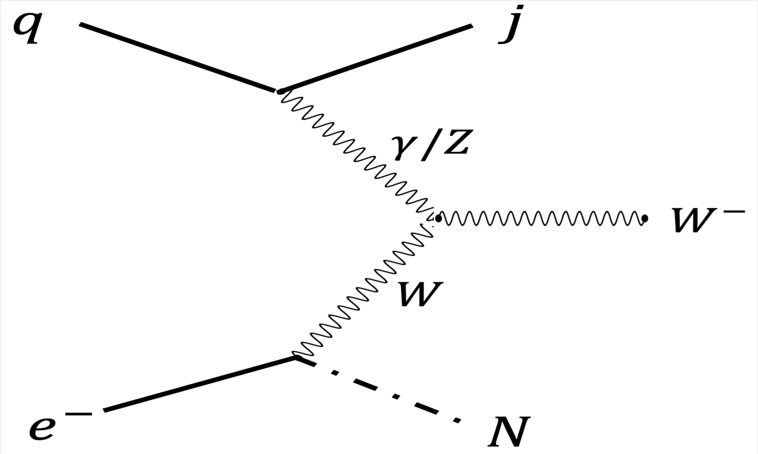

can confirm LNV
(need large $\sqrt{s}$)

Global Constraints

[Deppisch, Dev and Pilaftsis, New J. Phys. 17 (2015) 085019]

m_N: 0.1 ~ 500 GeV

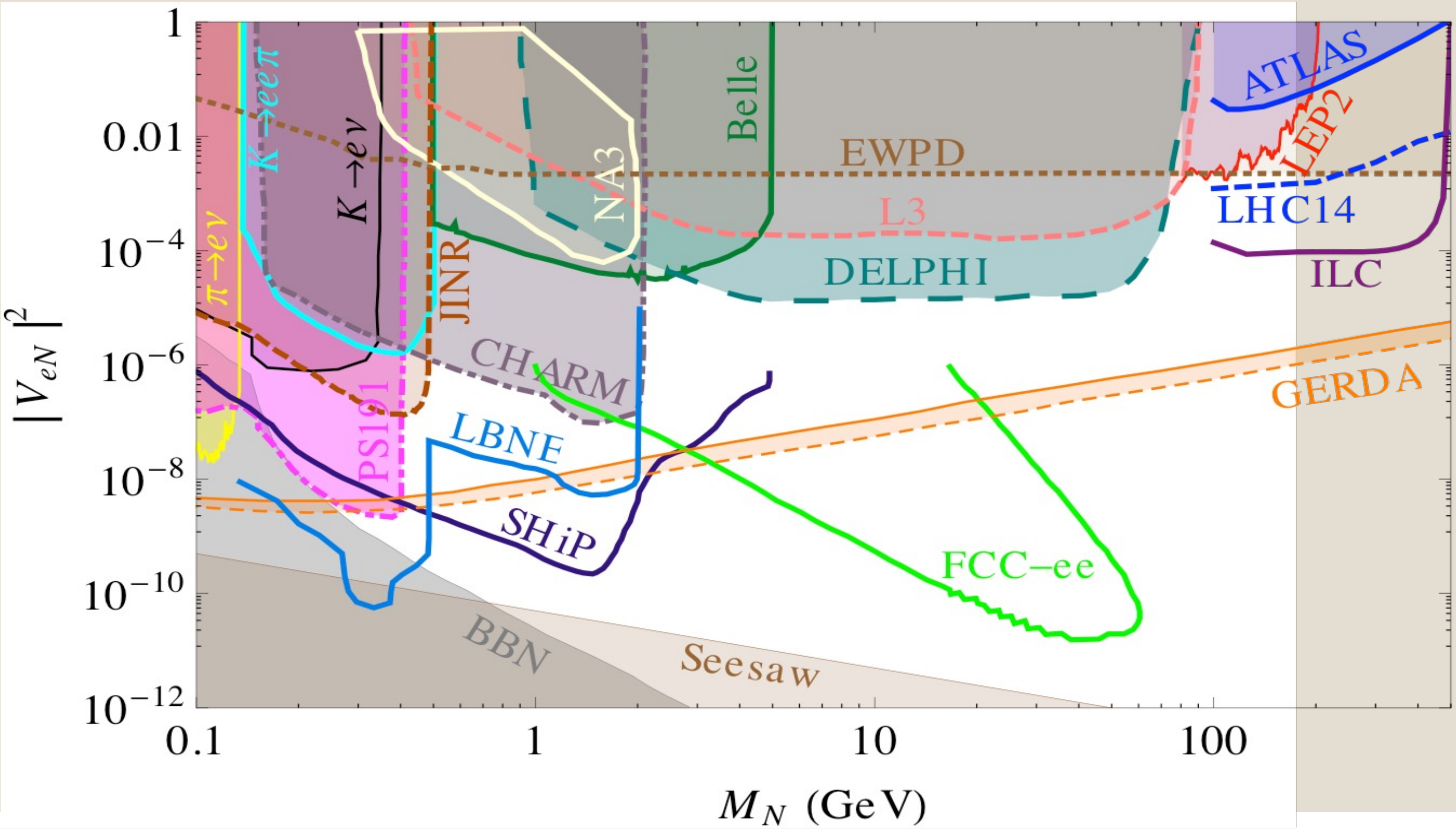

Collider Limits on $|V_{lN}|^2$

[H. Gu and **K. Wang**, PRD 106 (2022) no. 1, 015006]

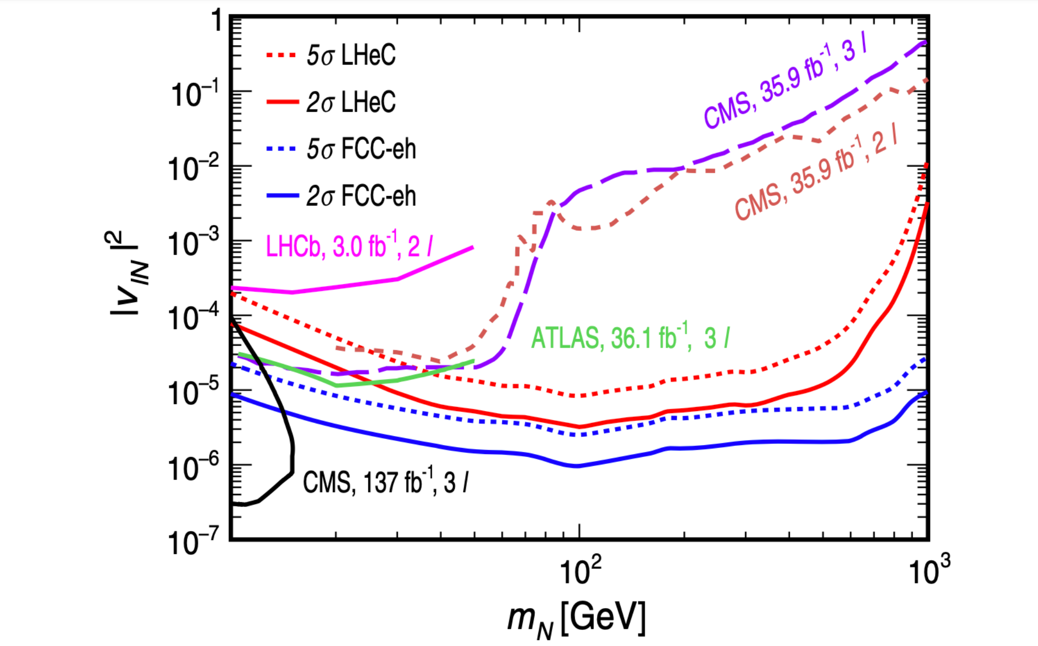

FIG. 5. 2σ and 5σ limits on mixing parameter $|V_{\ell N}|^2$ for the heavy neutrino mass in the range of 10–1000 GeV at the LHeC and FCC-eh. Also shown are the current experimental limits at 95% confidence level from the trilepton searches (CMS, 35.9 fb^{-1}, 3ℓ [24], CMS, 137 fb^{-1}, 3ℓ [26], and ATLAS, 36.1 fb^{-1}, 3ℓ [27]) and dilepton searches (CMS, 35.9 fb^{-1}, 2ℓ [25] and LHCb, 3.0 fb^{-1}, 2ℓ [28]) at the LHC.

$$|V_{\ell N}|^2 = |V_{eN}|^2 = |V_{\mu N}|^2$$

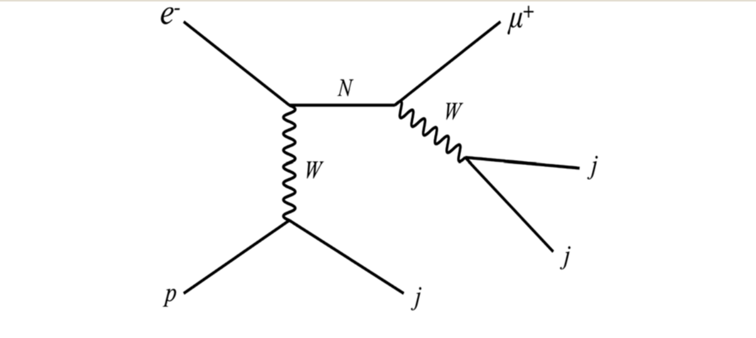

FIG. 1. The production process of the LNV signal via a Majorana heavy neutrino N at ep colliders.

Collider Limits on $|V_{\tau N}|^2$

[H. Gu, Y. Mao, H. Sun and **K. Wang**, JHEP 09 (2023) 152]

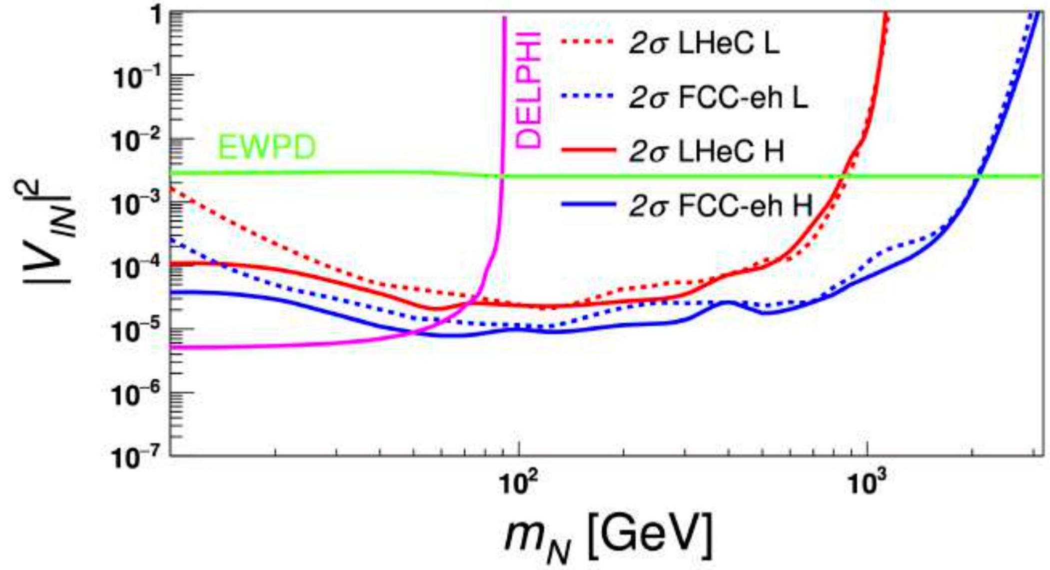

Figure 8. Assuming the mixing parameter $|V_{\ell N}|^2 = |V_{\tau N}|^2 = |V_{eN}|^2$, the discovery sensitivities on $|V_{\ell N}|^2$ at 2-σ significance as the heavy neutrino mass changes from 10 to 3000 GeV for Hadronic τ_h (H) and Leptonic τ_μ (L) final states at the LHeC and FCC-eh. The constraints from EWPD [47–51, 53] (green solid line) and DELPHI experiments [46] (purple solid line) are derived and displayed in the same plot for the comparison, see more details in appendix A.

$$|V_{\tau N}|^2 = |V_{eN}|^2 = |V_{\ell N}|^2$$

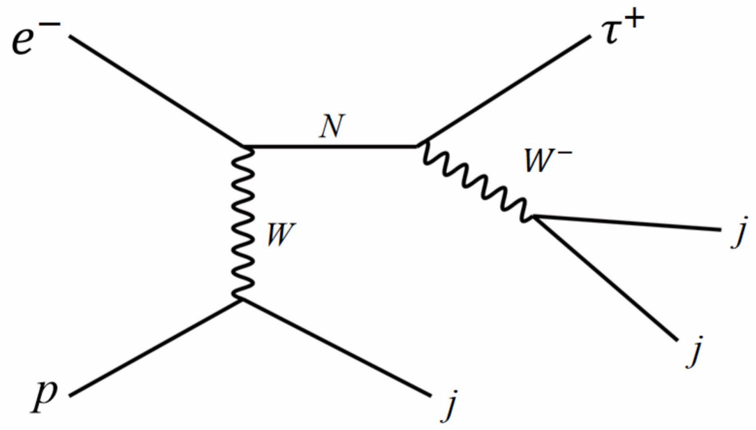

Near Detector @ LHC

[K. Cheung, **K. Wang**, and Z. S. Wang, JHEP 09 (2021) 026]

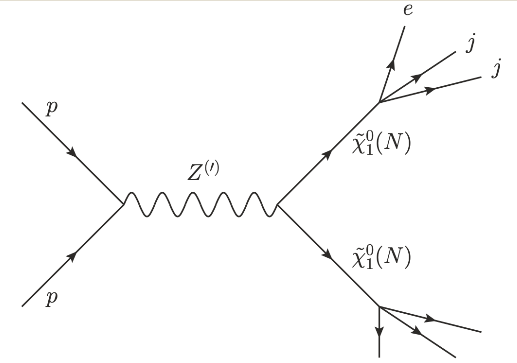

Figure 4. Feynman diagram of the signatures. We require at least one neutralino or HNL to decay into the ejj final state, as well as one hard prompt ISR jet in the event analysis.

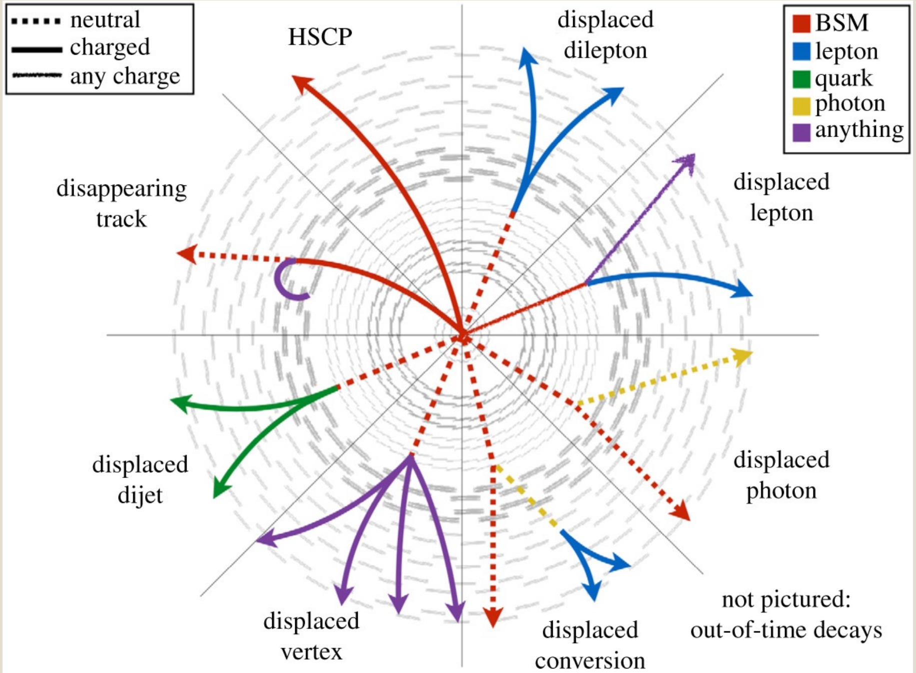

Signal rate

$$N_s^N = \sigma^N \cdot \mathcal{L} \cdot \mathrm{Br}(N \to ejj) \cdot 2 \cdot \epsilon^N, \tag{4.2}$$

where $N^Z \simeq 1.9 \times 10^{11}$ is the total number of Z-bosons resonantly produced with 3 ab^{-1} integrated luminosity [78], σ^N is the *inclusive* scattering cross section of $pp \to Z' \to NN$ calculated by MadGraph5 at the leading order (see the right plot of figure 2), and $\epsilon^{\tilde{\chi}_1^0}$ and ϵ^N are the event acceptance rates including the requirement of one hard ISR prompt jet. $\mathrm{Br}(\tilde{\chi}_1^0 \to e^- u\bar{s} \text{ or } e^+\bar{u}s) = 0.5$,[3] and $\mathcal{L} = 3$ ab^{-1} labels the integrated luminosity at the HL-LHC. Finally, the factor 2 that appears in both eq. (4.1) and eq. (4.2) accounts for the fact that in each signal event a pair of LLPs are produced and we require only one of them to decay into the specified final states.

Key observable: timing information

The time delay, Δt, is computed as follows,

$$\Delta t = t^e_{\text{arrival}} - t^e_{\text{prompt}}, \tag{3.1}$$

where $t^e_{\text{arrival}} = \frac{l_{\text{LLP}}}{\beta_{\text{LLP}}} + l_e$ is the arrival time of the electron at the MTD, with l_{LLP} (l_e) being the distance traveled by the LLP (displaced electron) before the LLP decays (the electron hits the MTD), and β_{LLP} being the speed of the LLP, while t^e_{prompt} is the time when the electron would arrive at the same position, *had it been promptly produced at the IP and traveling with the speed of light.*

Near Detector @ LHC

[K. Cheung, **K. Wang**, and Z. S. Wang, JHEP 09 (2021) 026]

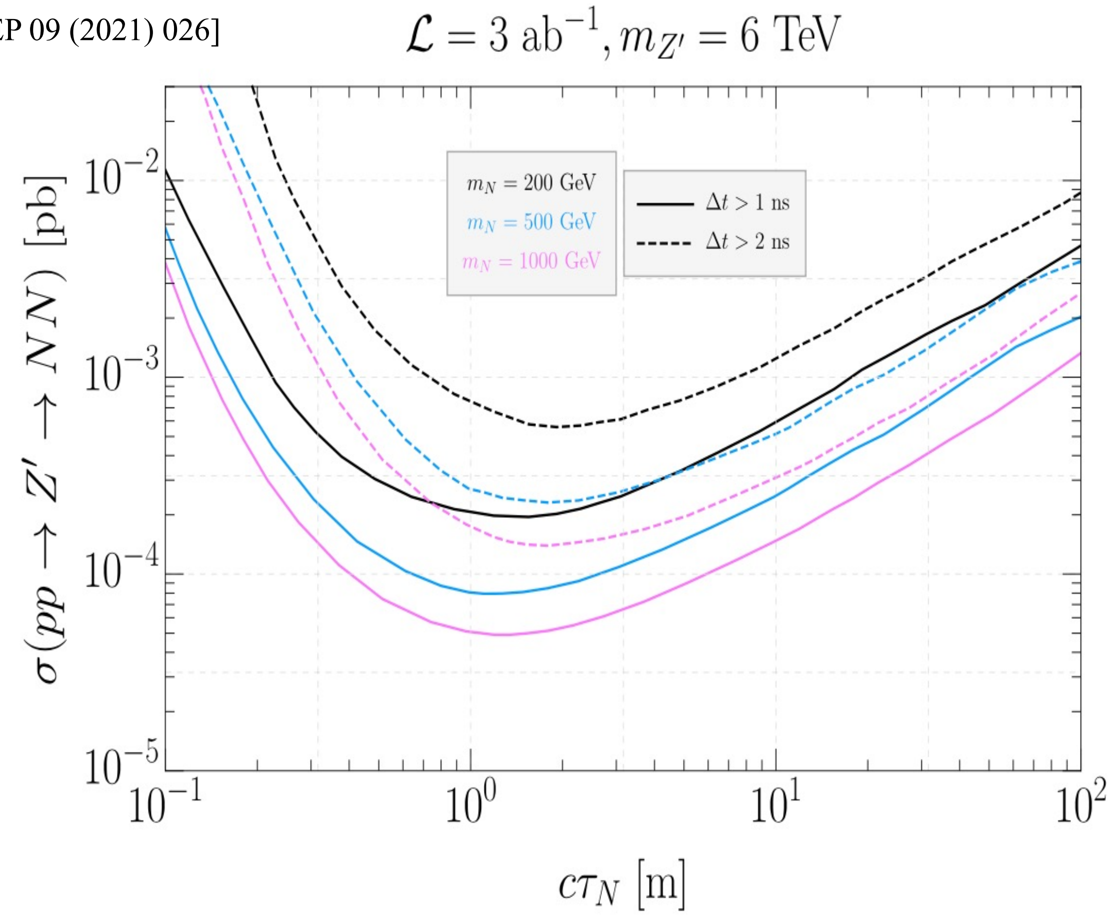

Figure 12. 95% C.L. exclusion limits on σ^N when varying $c\tau_N$, for $m_N = 200, 500,$ and $1000\,\text{GeV}$.

Far Detector @ LHC

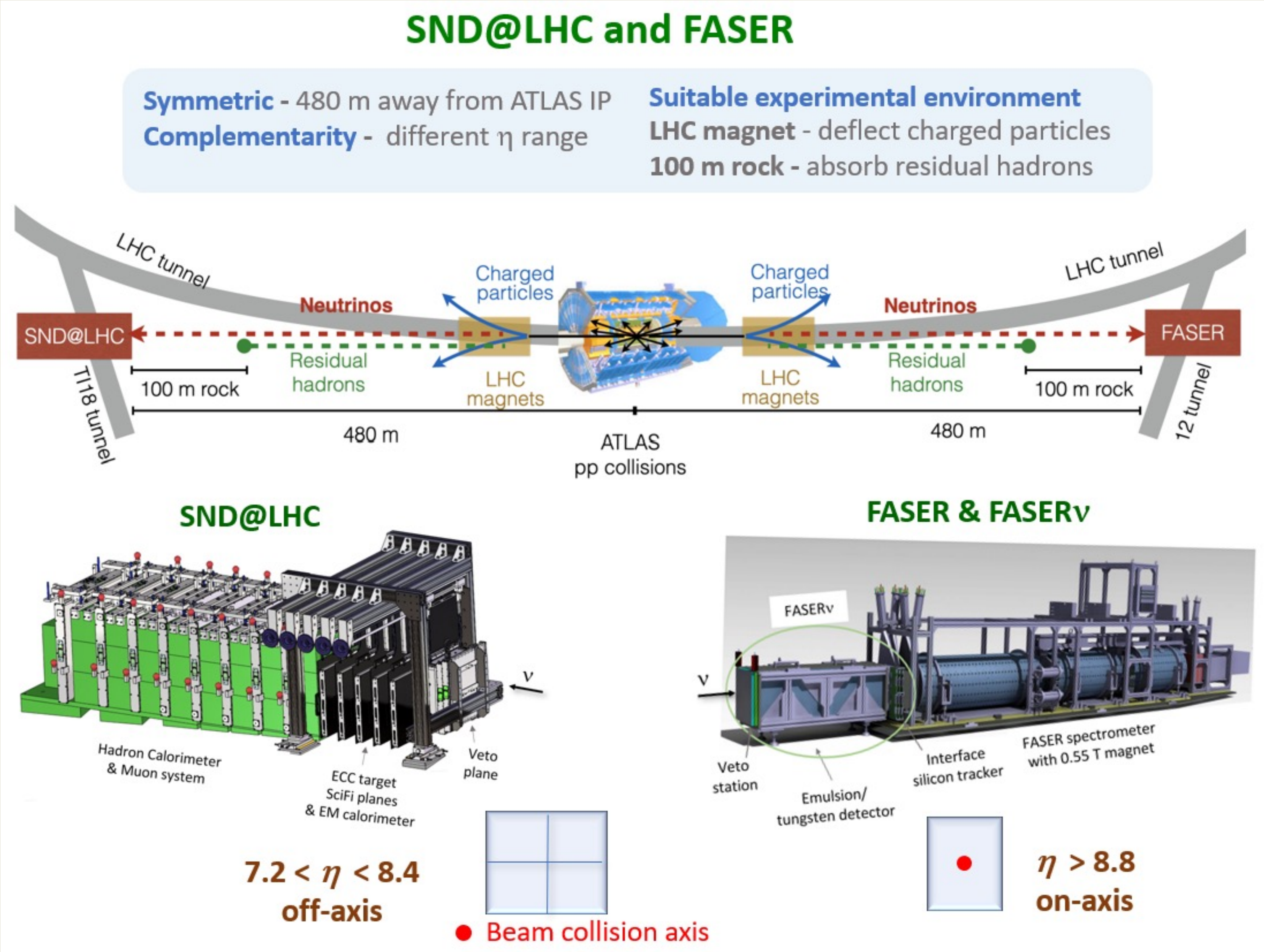

Current running FD experiments @ LHC

[http://www.ship-korea.com/SND.html]

[https://faser.web.cern.ch/index.php/]

[https://snd-lhc.web.cern.ch/]

[2210.02784, SND@LHC: The Scattering and Neutrino Detector at the LHC]

Far Detector @ LHC

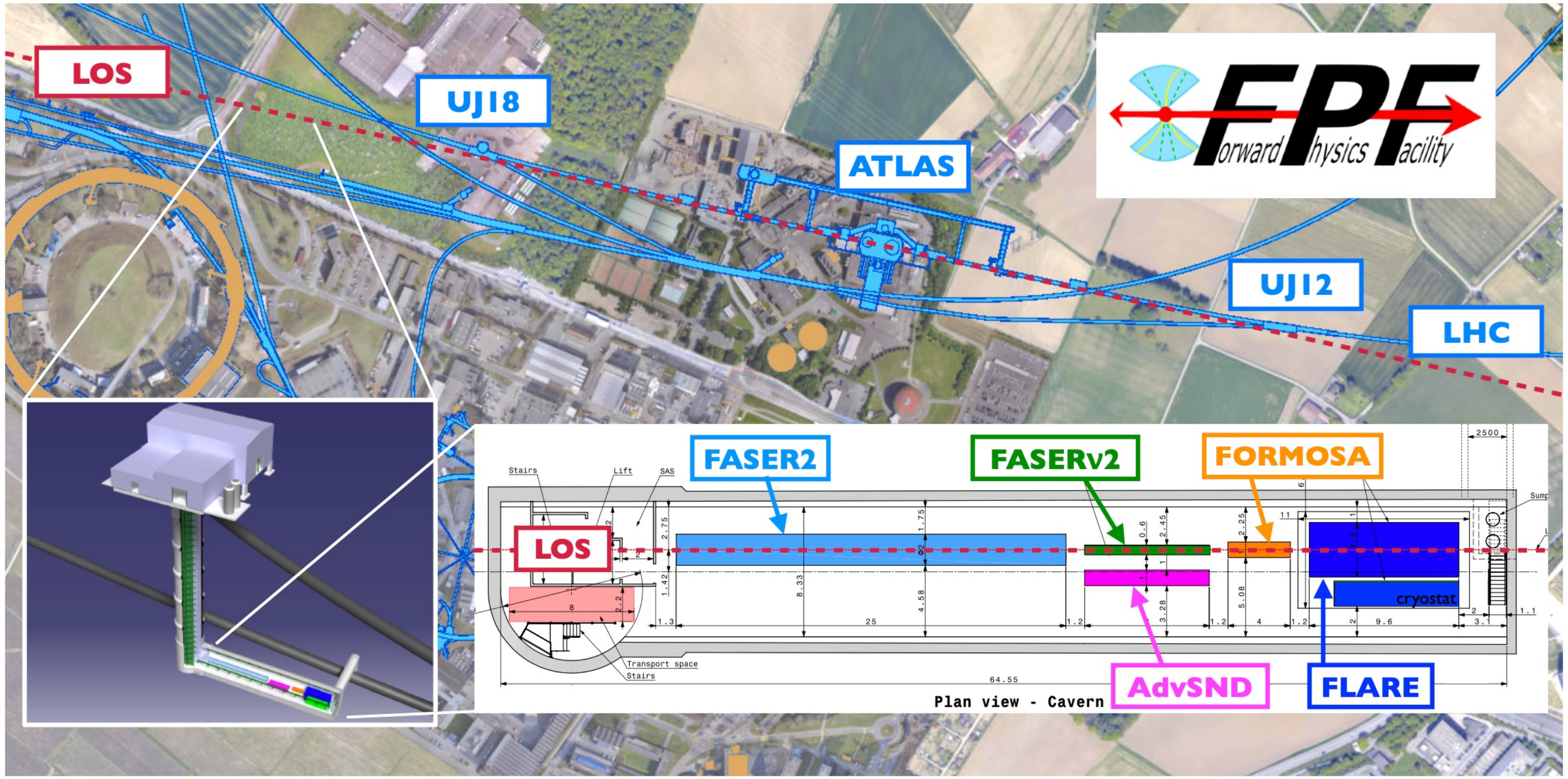

Figure 1: The preferred location for the Forward Physics Facility, a proposed new cavern for the High-Luminosity era. The FPF will be 65 m-long and 8.5 m-wide and will house a diverse set of experiments to explore the many physics opportunities in the far-forward region.

Proposed FD experiments：
MATHUSLA; FASER2, FASERv2, AdvSND, FLArE, FORMOSA；CODEX-b；AL3X; ...

[2203.05090, The Forward Physics Facility at the High-Luminosity LHC]

Far Detector @ LHC

Signal & Sensitivities for *N*

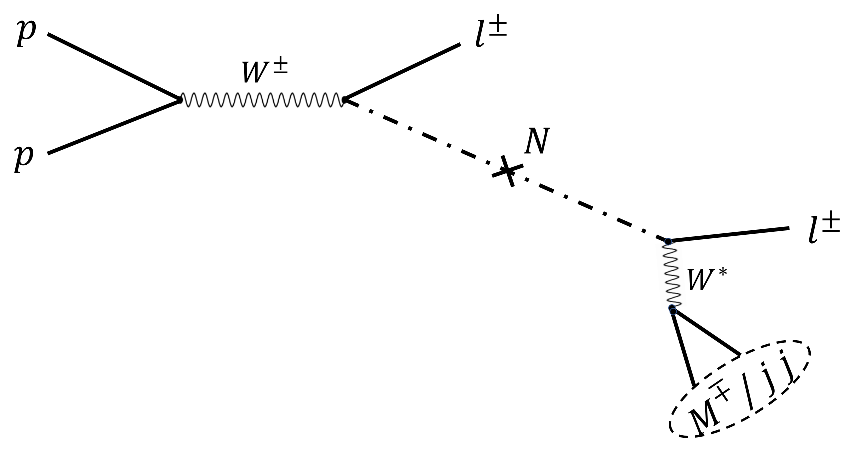

$$N_S^N = \frac{\sigma_\nu}{\mathrm{BR}(W \to e\,\nu)} \cdot \mathrm{BR}(W^\pm \to e^\pm N) \cdot \mathcal{L} \cdot \epsilon_{\rm trigger} \cdot \langle P_{\rm decay} \rangle \cdot \mathrm{BR}(N \to e^\pm jj/M^\mp)$$

[Y. Mao, **K. Wang** and Z. S. Wang, arXiv: 2305.03908]

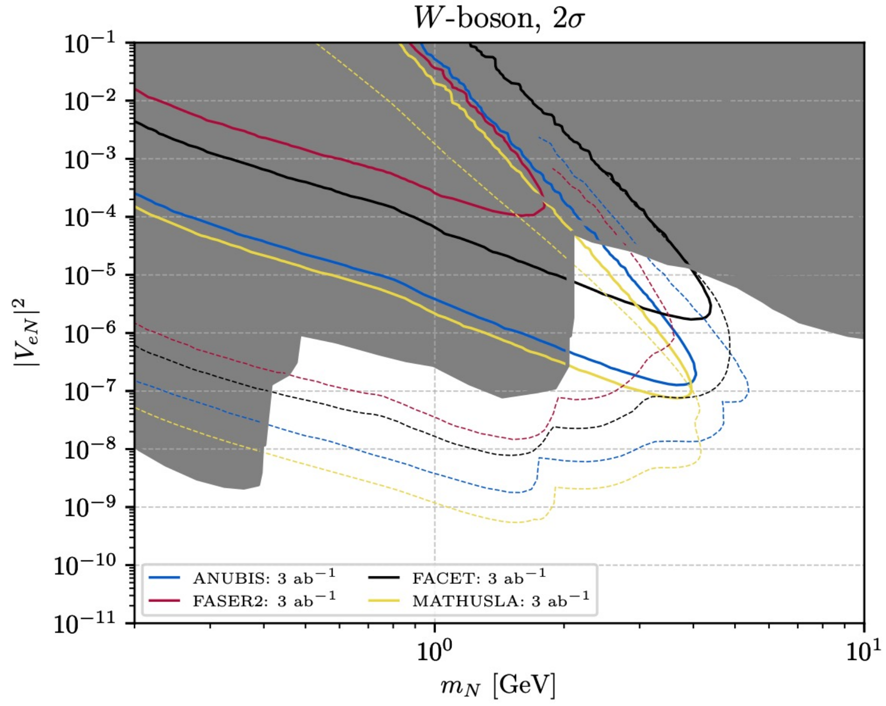

Figure 3. 2σ exclusion-bound plot for the displaced-vertex search associated with same-sign prompt and displaced leptons, produced from a W-boson decay at the IP and from the N decay in the far detectors, respectively. The gray area is the currently excluded parameter region, extracted from Refs. [102–106]. The solid lines are the sensitivity reach of the considered experiments with the LNV searches from this study, while the dashed lines correspond to inclusive displaced-vertex searches for HNLs produced from D and B-mesons' decays, as well as W-boson decays (important for ANUBIS and MATHUSLA only), extracted from Refs. [56, 58, 107]. We emphasize that the latter results cannot confirm LNV of the signal events and hence determine the Majorana nature of the HNLs.

Far Detector @ LHC

Signal & Sensitivities for SM ν

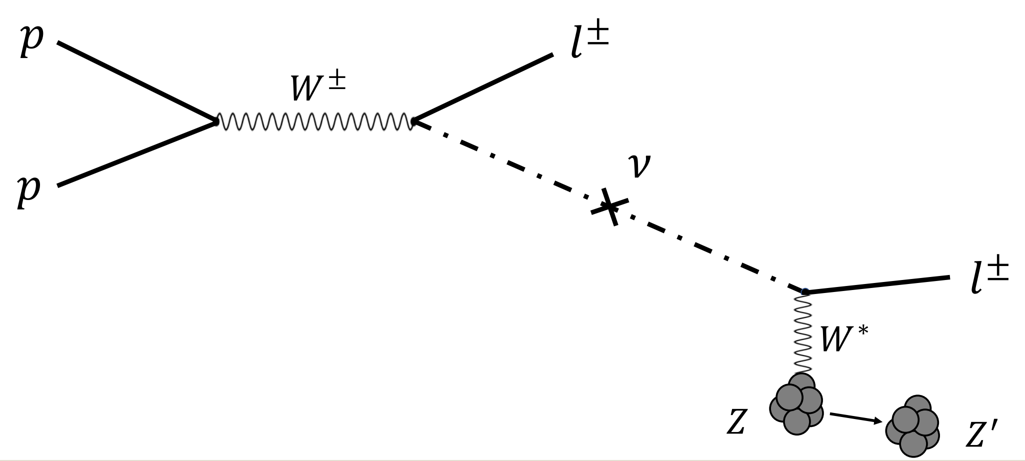

[Y. Mao, **K. Wang** and Z. S. Wang, arXiv: 2305.03908]

N_S^ν	e^+	e^-	μ^+	μ^-
FASERν	1.1×10^{-32}	7.0×10^{-32}	3.1×10^{-32}	3.4×10^{-32}
SND@LHC	7.5×10^{-32}	9.0×10^{-32}	7.6×10^{-32}	8.4×10^{-32}
FASERν2	1.5×10^{-30}	9.1×10^{-31}	4.1×10^{-30}	4.4×10^{-30}
AdvSND(far)	2.6×10^{-30}	3.1×10^{-30}	2.6×10^{-30}	2.9×10^{-30}
FLArE-10	7.6×10^{-31}	3.1×10^{-30}	1.6×10^{-30}	1.7×10^{-30}
FLArE-100	1.8×10^{-29}	2.0×10^{-29}	1.5×10^{-29}	1.8×10^{-29}

Table 3. Table of numerical results of N_S^ν at the neutrino detectors, for light neutrinos' both production and scattering with the SM CC interactions.

$$N_S^\nu = \sigma_\nu \cdot \mathcal{L} \cdot \epsilon_{\text{trigger}} \cdot \epsilon_{\text{window}} \cdot \langle \epsilon_{\text{h. f.}} \cdot P_{\text{scatt.}} \rangle$$

interaction probability of a neutrino with the detector

$$P_{\text{scatt.}} = \frac{\sigma_{\nu Z}}{A} \frac{m_{\text{det}}}{m_Z}$$

helicity flip suppression [Ben Jones, 2108.09364]

$$m_\nu^2/(4E_\nu^2) \sim 2.5\times10^{-25}$$

Only method to confirm LNV / Majorana nature of ν at colliders !

Far Detector @ LHC

Signal & Sensitivities for SM ν with EFT Operator

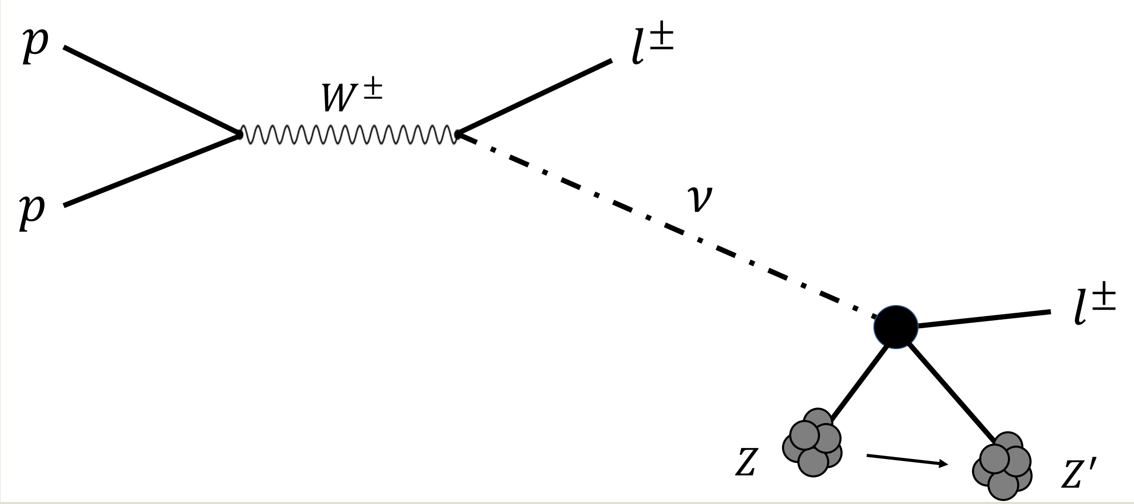

$$N_S^{\nu} = \sigma_{\nu} \cdot \mathcal{L} \cdot \epsilon_{\text{trigger}} \cdot \epsilon_{\text{window}} \cdot \langle \epsilon_{\text{h. f.}} \cdot P_{\text{scatt.}} \rangle$$

larger than four. A general framework with such operators including the neutrinos is known as the Standard Model Effective Field Theory (SMEFT) (see Ref. [91] for a review). In particular, SMEFT higher-dimensional operators which are LNV and include two quarks, one charged lepton, and a neutrino, arise at mass dimension 7 [92, 93].[4] Here, we focus on the operator $\epsilon_{ij}(L^i C\gamma_\mu e)(\bar{d}\gamma^\mu u)H^j$ with Wilson coefficient labeled as $1/\Lambda^3$, where H is the Higgs doublet, ϵ_{ij} is the $SU(2)$ index tensor, C is the Dirac charge conjugation matrix, Λ denotes the new-physics scale, leading to the neutrino-nucleus scattering into an electron

[Y. Mao, **K. Wang** and Z. S. Wang, arXiv: 2305.03908]

N_S^{ν}	e^+	e^-	μ^+	μ^-
FASERν	1.5×10^{-14}	8.5×10^{-15}	7.7×10^{-15}	2.0×10^{-15}
SND@LHC	2.2×10^{-14}	1.5×10^{-14}	3.7×10^{-14}	9.3×10^{-15}
FASERν2	2.0×10^{-12}	1.3×10^{-12}	1.0×10^{-12}	2.4×10^{-13}
AdvSND(far)	7.7×10^{-13}	5.0×10^{-13}	1.2×10^{-12}	2.1×10^{-13}
FLArE-10	6.6×10^{-13}	3.6×10^{-13}	1.0×10^{-12}	4.6×10^{-14}
FLArE-100	6.2×10^{-12}	2.9×10^{-12}	8.5×10^{-12}	1.3×10^{-12}

Table 4. Table of numerical results of N_S^{ν} for light neutrino produced via an s-channel W-boson decay and scattering via the dim-7 LNV operator $\epsilon_{ij}(L^i C\gamma_\mu e)(\bar{d}\gamma^\mu u)H^j$ with a coefficient $1/\Lambda^3 \sim 1/(5\ \text{TeV})^3$, where the neutrino helicity flip is not included.

Only method to confirm LNV / Majorana nature of ν at colliders !

Far Detector @ CEPC

[Zeren Simon Wang, **K. Wang**, PRD 101 (2020) no.7, 075046]

scenario		$Z \to N\nu$	
LLP		N	
production $e^-e^+ \to$		Z	
$\sqrt{s}$ [GeV]		91.2	
N_h	CEPC	-	
	FCC-ee		
N_Z	CEPC	7.0×10^{11} [16]	16 ab^{-1}, 2 years, 2 IPs
	FCC-ee	5.0×10^{12} [20]	150 ab^{-1}, 4 years, 2 IPs

Signal Production

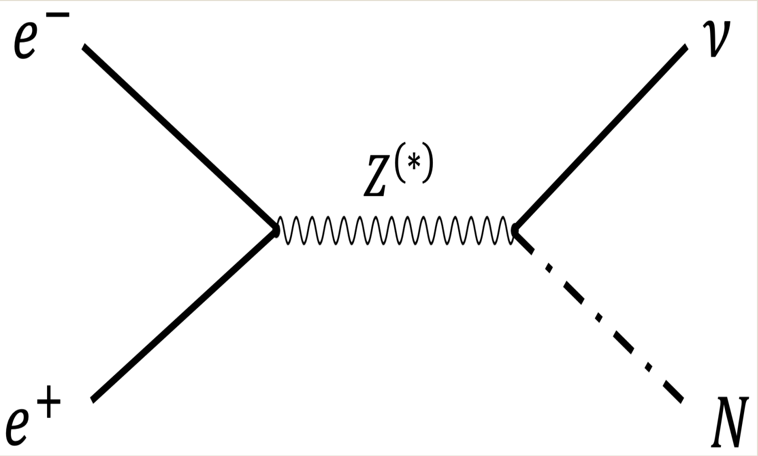

Far Detector @ CEPC

Kinematical Distributions

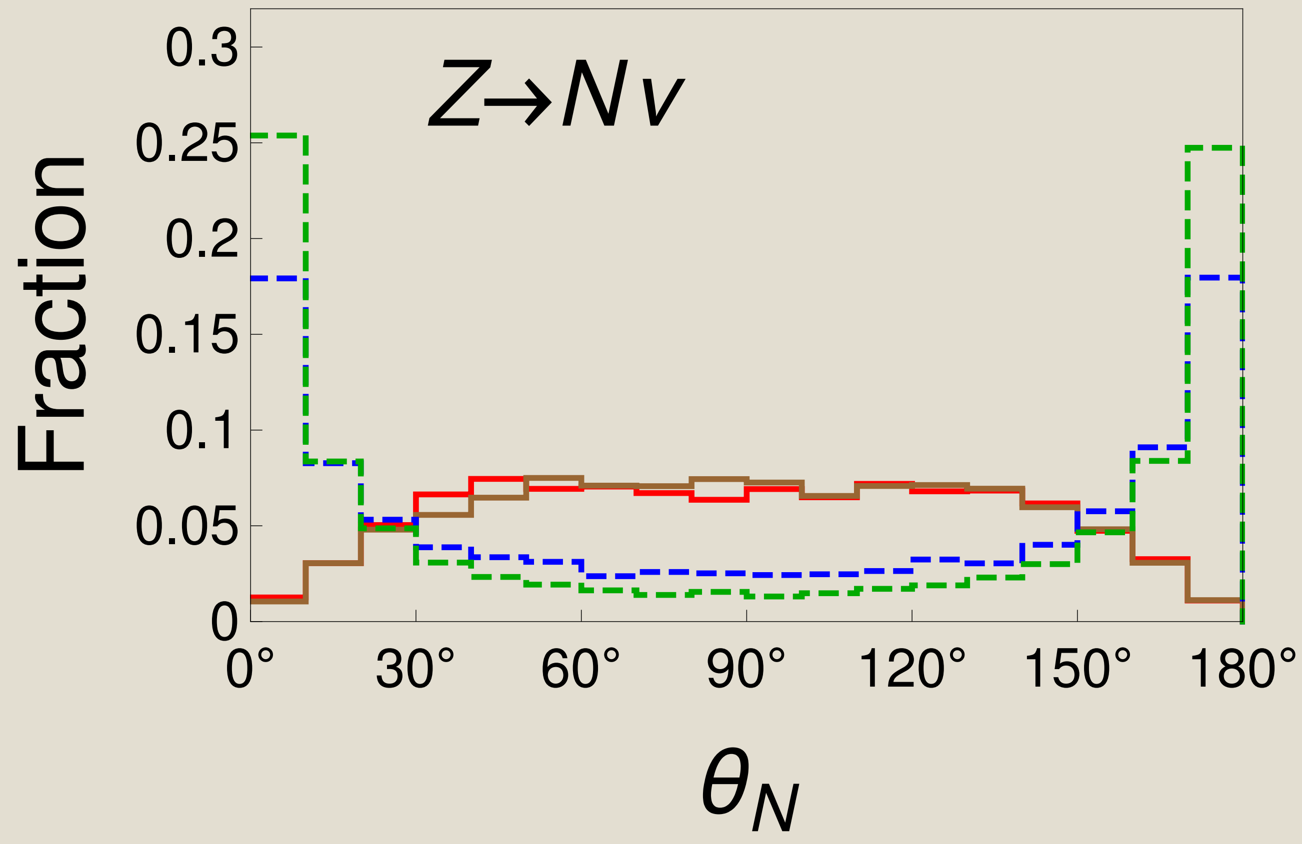

@ pp: very forward direction
@ ee: more in the transverse direction

FDs in the very forward direction like FASER may not work at ee colliders.
Better to be installed in the central region.

Far Detector @ CEPC

Detector Designs

	V [m^3]	B [m]	H [m]	L [m]	(x_1, y_1, z_1) [m]	(x_2, y_2, z_2) [m]	D [m]
FD1	5.0×10^3	10	10	50	(5, -5, -25)	(15, 5, 25)	5
					(10, -5, -25)	(20, 5, 25)	10
FD2	8.0×10^5	200	20	200	(-100, 50, 50)	(100, 70, 250)	50
					(-100, 100, 100)	(100, 120, 300)	100
FD3	8.0×10^5	200	20	200	(-100, 50, -100)	(100, 70, 100)	50
					(-100, 100, -100)	(100, 120, 100)	100
FD4	8.0×10^5	100	80	100	(-50, 50, -50)	(50, 130, 50)	50
					(-50, 100, -50)	(50, 180, 50)	100
FD5	3.2×10^6	200	80	200	(-100, 50, -100)	(100, 130, 100)	50
					(-100, 100, -100)	(100, 180, 100)	100
FD6	8.0×10^7	1000	80	1000	(-500, 50, -500)	(500, 130, 500)	50
					(-500, 100, -500)	(500, 180, 500)	100
FD7	8.0×10^5	2000	20	20	(-1000, 50, -10)	(1000, 70, 10)	50
					(-1000, 100, -10)	(1000, 120, 10)	100
FD8	8.0×10^5	20	20	2000	(-10, 50, -1000)	(10, 70, 1000)	50
					(-10, 100, -1000)	(10, 120, 1000)	100

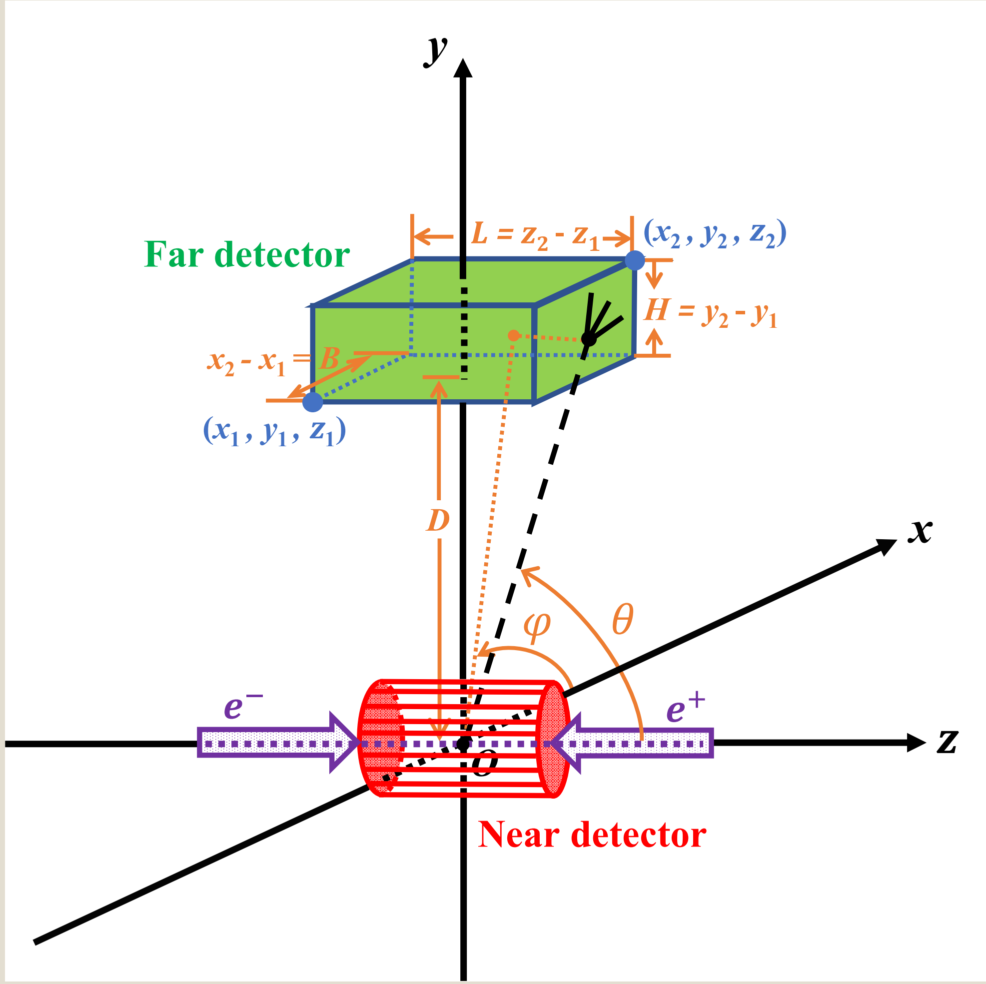

Simple shape: cuboid, similar to MUTHUSLA
Varying: position & geometry size

Far Detector @ CEPC

$Z \to N\nu$ @ $\sqrt{s} = 91.2$ GeV

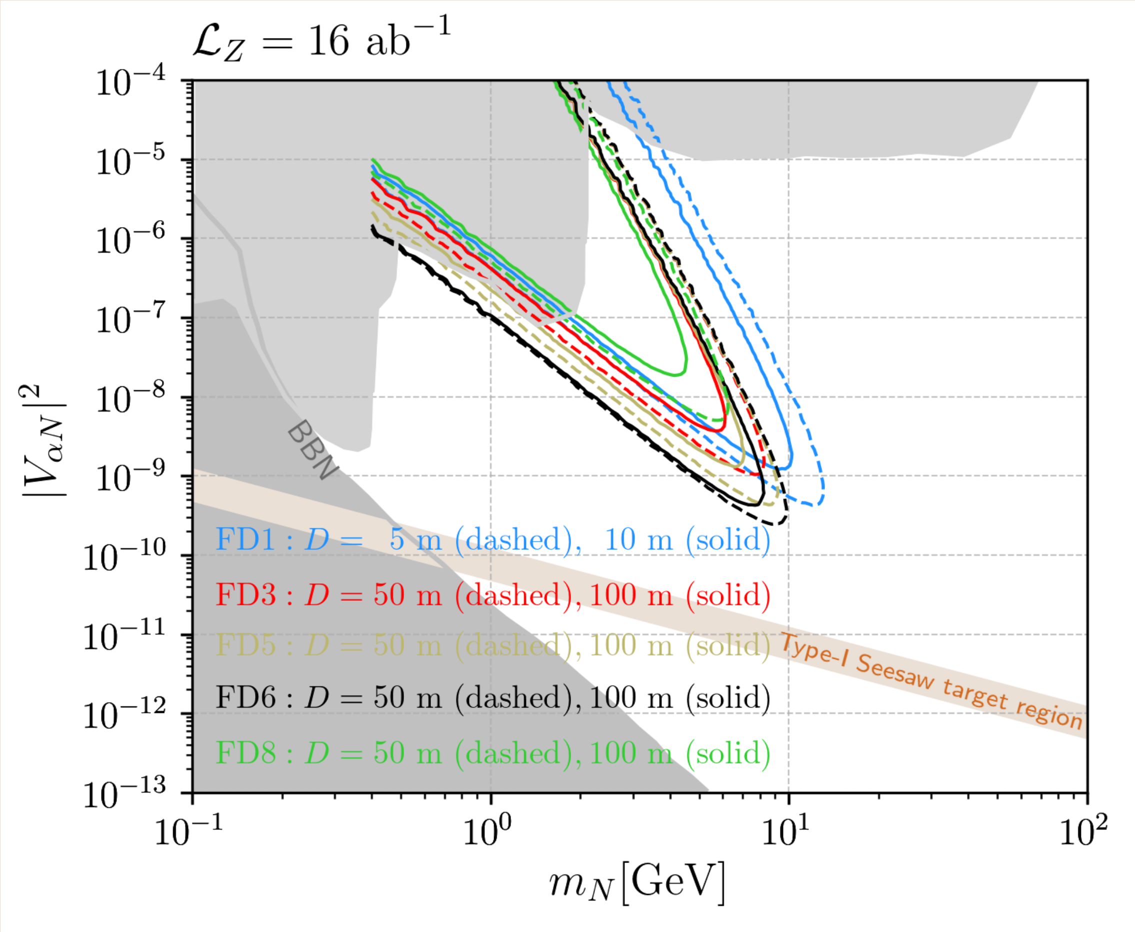

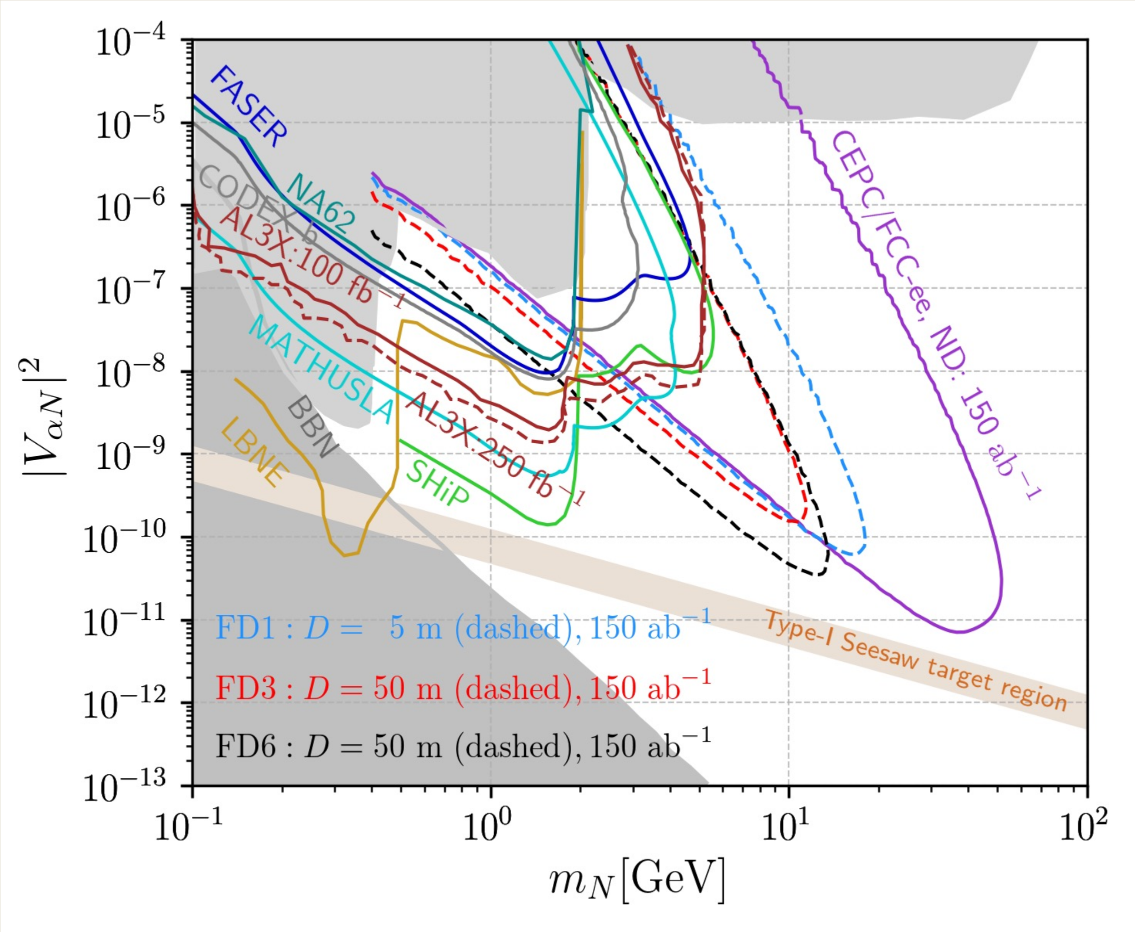

Far Detector @ CEPC

$Z \to N\nu$ @ $\sqrt{s} = 91.2$ GeV

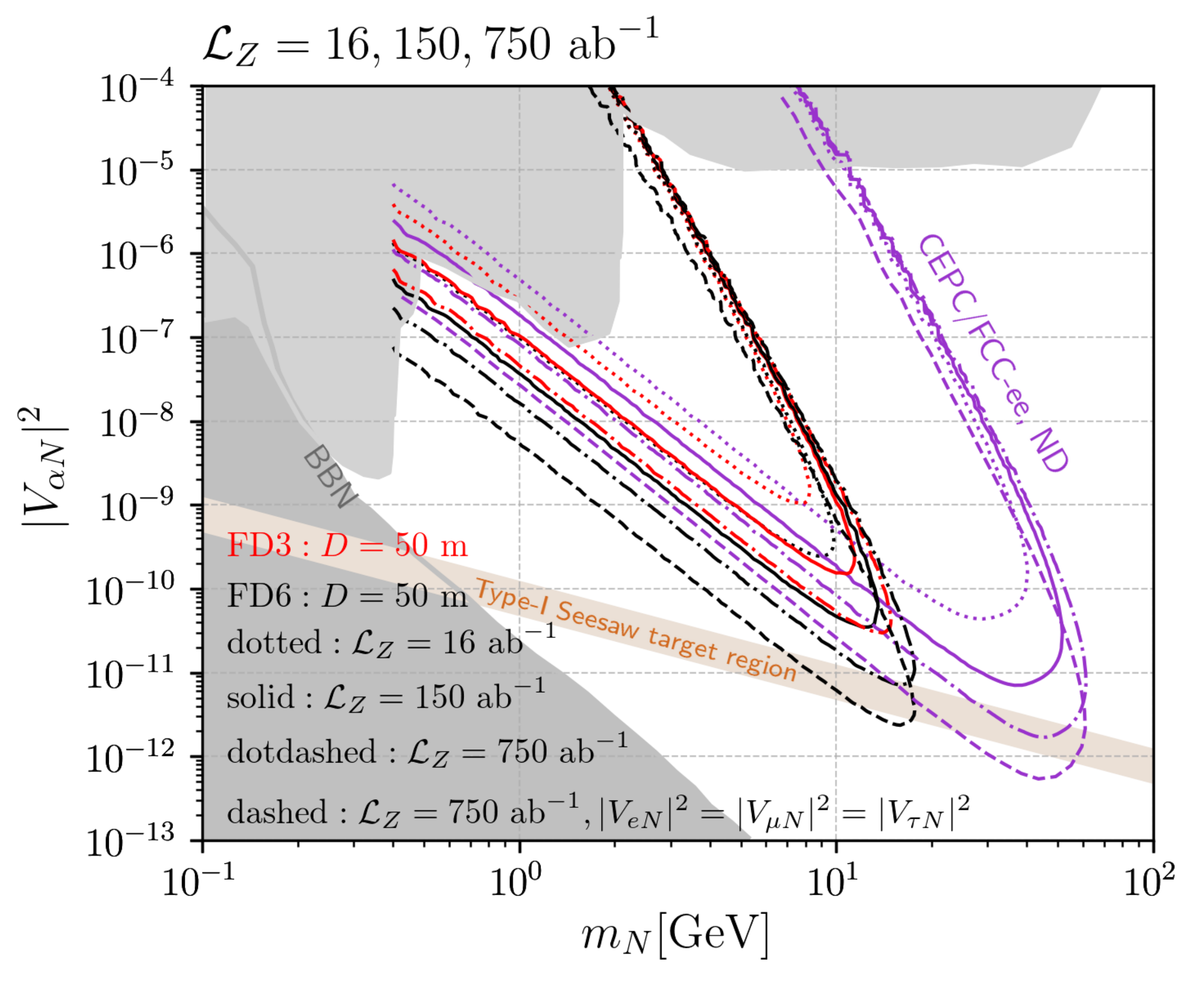

750 ab^{-1}, 10 years, 4 IPs;
or to increase the instantaneous luminosity;
or to relax the theoretical assumptions

Can test the Type-I seesaw directly!

Discussion

LL *N* searches @ colliders are important ways to BSM physics.

Studies with near detectors and far detectors.

LLP searches with near detector @ BESIII ?

→ Good physics models / signals ?

LLP searches with far detector @ BESIII ?

→ Location ? (need cavern)

→ Technology: timing / track resol.

Discussion

Neutrino Production @ LHC

Table 1 Decays considered for the estimate of forward neutrino production. For each type in the first column, we list the considered particles in the second column and the main decay modes contributing to neutrino production in the third column. In the last four columns we show which generators were used to obtain the meson spectra: EPOS- LHC (E) [59], QGSJET- II- 04 (Q) [60], SIBYLL 2.3C (S) [61–64], and PYTHIA 8 (P) [66,67], using both the MONASH-tune [68] and the minimum bias A2-tune [69]

Type	Particles	Main decays	E	Q	S	P
Pions	π^+	$\pi^+ \to \mu\nu$	✓	✓	✓	–
Kaons	K^+, K_S, K_L	$K^+ \to \mu\nu,\ K \to \pi\ell\nu$	✓	✓	✓	–
Hyperons	$\Lambda, \Sigma^+, \Sigma^-, \Xi^0, \Xi^-, \Omega^-$	$\Lambda \to p\ell\nu$	✓	✓	✓	–
Charm	$D^+, D^0, D_s, \Lambda_c, \Xi_c^0, \Xi_c^+$	$D \to K\ell\nu,\ D_s \to \tau\nu,\ \Lambda_c \to \Lambda\ell\nu$	–	–	✓	✓
Bottom	$B^+, B^0, B_s, \Lambda_b, \ldots$	$B \to D\ell\nu,\ \Lambda_b \to \Lambda_c\ell\nu$	–	–	–	✓

tom (light green) decays. The two-body decays of charged pions $\pi^\pm \to \mu\nu_\mu$ and kaons $K^\pm \to \mu\nu_\mu$ are the dominant sources of ν_μ production. Note that kaon decays provide a larger contribution at higher energies due to the larger fraction of the parent meson energy obtained by the neutrino in kaon decays. Electron neutrinos are predominantly produced in three-body kaon decays $K \to \pi e\nu_e$, with $K^\pm$, K_L, and K_S providing similar contributions.

neutrino detectors	material	A [cm^2]	$m_{\rm det}$ [ton]	$\eta_{\rm min}$	$\eta_{\rm max}$	$\mathcal{L}$ [fb^{-1}]
FASERν [35, 71, 72]	tungsten	25 × 25	1.2	8.5	∞	150
SND@LHC [36, 37]	tungsten	40 × 40	0.85	7.2	8.4	150
FASERν2 [40]	tungsten	40 × 40	20	8.5	∞	3000
AdvSND(far) [40, 41]	tungsten	100 × 55	5	7.2	8.4	3000
FLArE-10 [40, 42]	liquid argon	100 × 100	10	7.5	∞	3000
FLArE-100 [40, 42]	liquid argon	160 × 160	100	7	∞	3000

Table 1. Summary of neutrino detectors at the LHC. We list the material type, area A, detector mass $m_{\rm det.}$, minimal and maximal pseudorapidity coverage $\eta_{\rm min}$ and $\eta_{\rm max}$, as well as the corresponding integrated luminosity, $\mathcal{L}$, for each detector.

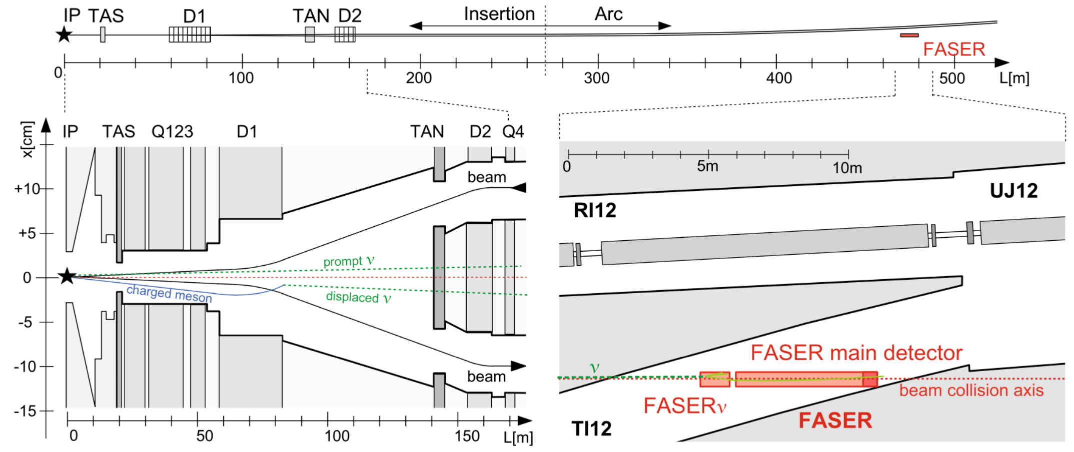

Fig. 1 Schematic view of the far-forward region downstream of ATLAS. *Upper panel*: FASER is located 480 m downstream of ATLAS along the beam collision axis (dotted line) after the main LHC tunnel curves away. *Lower left panel*: High-energy particles produced at the IP in the far-forward direction. Charged particles (solid lines) are deflected by LHC quadrupole (Q) and dipole (D) magnets. Neutral hadrons are absorbed by either the TAS front quadrupole absorber or by the TAN neutral particle absorber. Neutrinos (dashed lines) are produced either promptly or displaced and pass through the LHC infrastructure without interacting. Note the extreme difference in horizontal and vertical scales. *Lower right panel*: Neutrinos may then travel ∼ 480 m further downstream into tunnel TI12 and interact in FASERν, which is located at the front of the FASER main detector

Table 2 The expected number of neutrinos with $E_\nu > 100$ GeV interacting through CC processes in FASERν, the expected number of reconstructed vertices in FASERν requiring $n_{\rm tr} \geq 5$, and the mean energy of neutrinos that interact in FASERν. Here we assume a benchmark detector made of tungsten with dimensions 25 cm × 25 cm × 1 m at the 14 TeV LHC with an integrated luminosity of $L = 150\ \text{fb}^{-1}$. Reductions in the number of reconstructed vertices from the geometrical acceptance and lepton identification efficiency have not been included. The uncertainties correspond to the range of predictions obtained from different MC generators

	Number of CC interactions	Number of reconstructed vertices	Mean energy (GeV)
$\nu_e + \bar\nu_e$	1296^{+77}_{-58}	1037^{+52}_{-36}	827
$\nu_\mu + \bar\nu_\mu$	20439^{+1545}_{-2314}	15561^{+1103}_{-1514}	631
$\nu_\tau + \bar\nu_\tau$	$21^{+3.3}_{-2.9}$	$17^{+2.6}_{-2.6}$	965